Avoided criticality in near-optimally doped high-temperature superconductors

Kristjan Haule and Gabriel Kotliar

Department of Physics, Rutgers University, Piscataway, New Jersey 08854, USA

(Received 27 August 2007; published 24 September 2007)

We study the crossover from the underdoped to the overdoped regime of the *t-J* model within a plaquette dynamical mean field approach. We find that the shortest electron lifetime occurs near optimal doping where the superconducting critical temperature is maximal. The mean field theory provides a simple physical picture of this effect. In the underdoped regime, the charge carriers propagate coherently among spin singlets, formed by the superexchange interaction. In the overdoped, large carrier concentration regime, the Kondo effect dominates resulting in spin-charge composite quasiparticles which are also coherent. Separating these two Fermi liquid regimes, there is a critical doping where the superexchange and the Kondo interaction balance each other. At this point, the normal phase is highly incoherent and the optical conductivity exhibits power law behavior at intermediate frequencies. The onset of superconductivity restores coherence, causing the appearance of a resonance in the spin channel.

The *t-J* model is one of the simplest models of strongly correlated electron materials. It received significant attention over the past 20 years, following the proposal by Anderson that it should serve as a minimal model to describe the cuprate superconductors. In spite of decades of intensive work, exact results for this model in two dimensions are not available, and consensus on a clear physical picture of the physics described by this model is still lacking.

Over the past decade, significant progress in the field of correlated electrons was achieved through the development of the dynamical mean field theory. In its single site version, this method describes lattice models in terms of a single site impurity problem embedded in a medium. Cluster extensions of this method are currently a subject of intensive investigations[1–6] (for reviews, see Refs. [7] and [8]).

In this Brief Report, we apply cluster dynamical mean field theory (CDMFT) to construct a mean field theory of the *t-J* model. There are several motivations for constructing a mean field theory of the *t-J* model based on a dynamical plaquette. Mean field theory is needed to define and study the normal state underlying an ordered state. A mean field theory based on a plaquette describes the *d*-wave superconductivity, one of the leading candidates for a ground state of the *t-J* model. It describes on the same footing two roads for singlet formation: the Kondo effect, in which a spin can form a singlet with a bath of conduction electrons, and the superexchange mechanism, which locks two spins on a bond in a singlet state. It can also describe the metastable normal state below T_C. A clear understanding of the evolution of the different mean field states is an important step in understanding a model.

In this Brief Report, we study the crossover from underdoped to overdoped regime and find a surprising result: The point of maximal superconducting transition temperature in this model occurs where the underlying normal state has the shortest lifetime. The onset of superconductivity rapidly restores Fermi liquid coherence and gives rise to a resonance in the spin channel. Around this doping, the optical conductivity has an approximate power law at intermediate frequencies. Hence, various authors have hypothesized the existence of a hidden critical point under the superconducting dome.

Our starting point is the Hamiltonian

$$H = -\sum_{ij\sigma} t_{ij}c_{i\sigma}^{\dagger}c_{j\sigma} + \frac{1}{2}\sum_{ij} J_{ij}\mathbf{S}_i\mathbf{S}_j. \quad (1)$$

It contains two terms: the first describes the kinetic energy which delocalizes the holes introduced by doping, and the second represents spin-spin interaction. In this work, we took $J/t=0.3$. $c_{j\sigma}$ destroys projective fermions to enforce a constraint of no double occupancy. This constraint will be treated exactly in this work.

We use CDMFT to map this model into a plaquette (four impurity sites) embedded in a medium which obeys a self-consistency condition. We employed two different cluster schemes: a cellular dynamical mean field theory (DMFT) approach based on a real space perspective[9] and an extended dynamical cluster approximation, an approach derived from a momentum space perspective.[7] Our main conclusions are robust features of 2×2 CDMFT and were reached using both cluster schemes.

The impurity model consists of a cluster of four sites, a bath of noninteracting fermionic and bosonic particles, and a coupling between the bath and the cluster. It is convenient to introduce the cluster eigenstates defined by the exact diagonalization of the cluster Hamiltonian, i.e., $H_{cluster}|m\rangle = E_m|m\rangle$. To each cluster eigenstate, we associate a pseudoparticle creation operator $|m\rangle = a_m^{\dagger}|0\rangle$. The cluster part of the Hamiltonian is quadratic in the pseudoparticles, and the bath Hamiltonian is also noninteracting. A cubic term describes the interaction between the cluster and the bath. To solve the four-impurity problem, we use two different impurity solvers. The first is the noncrossing approximation (NCA) combined with the slave particle approach.[10] The second is a recently developed continuous time quantum Monte Carlo (CTQMC) method.[11,12] Both impurity solvers employ the diagrammatic expansion of the hybridization term. Within the noncrossing approximation, the crossing diagrams are neglected, but real frequency information is easily extracted while the quantum Monte Carlo method allows summation of all diagrams but works with imaginary time. All the qualitative conclusions can be reached by both methods. In this Brief Report, we focus on a physical description of the results; a more detailed presentation of the methodology
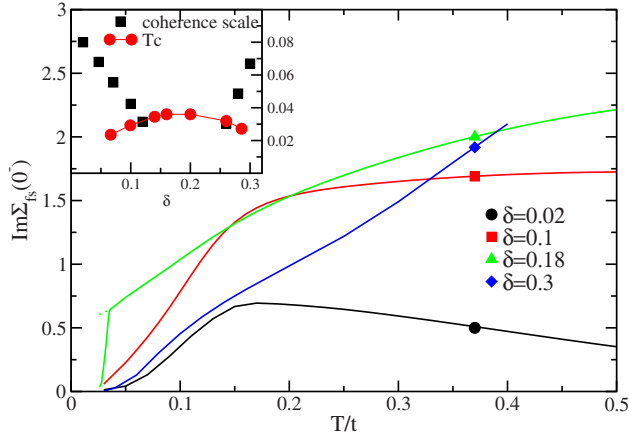
FIG. 1. (Color online) The cluster self-energy Σ_{fs} at zero frequency as a function of temperature for few doping levels obtained by NCA. The inset shows the estimation of the coherent scale in the normal state of the t-J model (black squares) and transition temperature to superconducting state (red dots). The coherence scale is extracted from the self-energy by fitting the parabolic Fermi liquid temperature profile, and the characteristic scale sets the coherence scale.

will be made available in a longer publication.

Physically, pseudoparticles represent coarse grained version of the important many-body excitations including fermionic quasiparticles and bosonic collective modes. They have quantum numbers describing their spin S, number of particles N (which, divided by the cluster size, gives the density), and a coarse grained momentum K. There are four cluster momenta: $(0,0)$, (π,π), $(\pi,0)$, and $(0,\pi)$. They are naturally defined in extended dynamical cluster approximation (EDCA) as representing different patches in momentum space and in CDMFT as cluster eigenvalues with a similar physical interpretation. We found that the spectral functions associated with $(0,0)$ and (π,π) are both gapped, so we focus in this Brief Report on the electron self-energy with cluster momenta $(\pi,0)$ and $(0,\pi)$ regions which contain the Fermi surface of the model in the underdoped and slightly overdoped regimes. We will denote this self-energy Σ_{fs} to stress that it is the cluster representative of the low energy fermionic degrees of freedom, which are relevant for thermodynamical and transport properties.

A striking indication for the existence of an anomaly near optimal doping comes from the evaluation of the electron scattering rate from the imaginary part of the electron self-energy as a function of temperature for few different doping levels. The NCA calculations of this quantity within EDCA are displayed in Fig. 1. At large and small doping, the scattering rate is small as expected for a Fermi liquid. Remarkably, it becomes very large in the region near optimal doping when the critical temperature is maximal. A coherence scale, estimated from the scattering rate, is plotted in the inset of Fig. 1 and shows that it tends to vanish close to the point of maximal superconducting transition temperature.

Figures 2(a) and 2(b) show the CTQMC results for the scattering rate versus doping in the real space version of CDMFT and confirm the incoherence of the optimally doped system. The imaginary part of the self-energy at the first
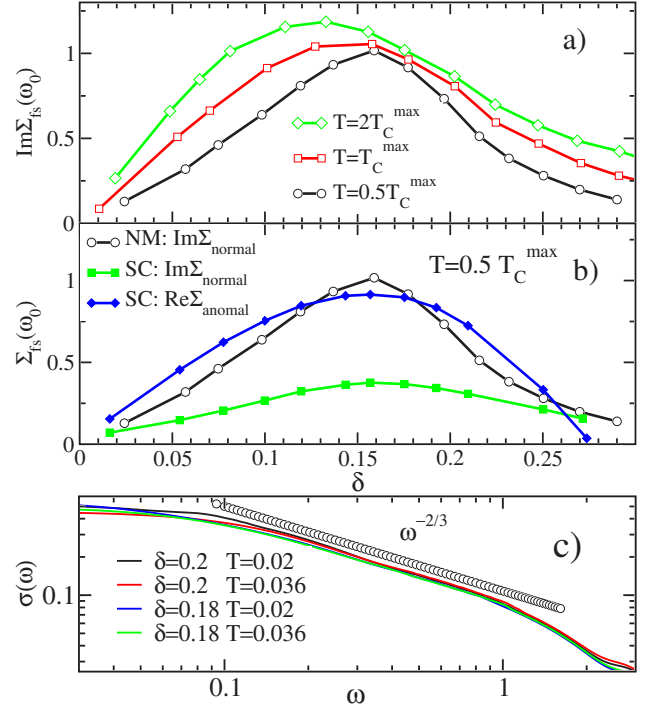

FIG. 2. (Color online) (a) Imaginary part of cluster self-energy Σ_{fs} at the lowest Matsubara frequency ω_0 versus doping for three different temperatures obtained by CTQMC (Ref. 12) within real space CDMFT. The scattering rate is peaked at optimal doping and $T_C^{max}=0.01t$. (b) The large imaginary part of the self-energy of the normal state (black circles) is severely reduced in superconducting state (green squares). The scattering rate is peaked at the point of maximal anomalous self-energy (blue diamonds) tracking the point of the highest T_C (obtained by CTQMC within real space CDMFT). (c) The optical conductivity $\sigma(\omega)$ is proportional to $\omega^{-2/3}$ in the intermediate frequency region for optimally doped system (obtained by NCA). Slightly away from the optimal doping, the power law remains valid in a narrower frequency region and is first cut off at low frequency.

Matsubara point is small for both the underdoped and overdoped systems, while it is peaked at optimal doping. The peak is slightly shifted with temperature and, if the normal state is continued below the superconducting transition temperature, the peak of scattering rate coincides with the maximum of the anomalous self-energy which traces the maximum of the transition temperature [see Fig. 2(b)]. Allowing off-diagonal superconducting long range order severely reduces the scattering rate, eliminating the traces of the underlying critical behavior, hence the name avoided criticality.

Further evidence for the anomaly at optimal doping comes from the power law behavior of the optical conductivity in the intermediate frequency regime, shown in Fig. 2(c). It follows an approximate power law with an exponent of 2/3 reminiscent of the experimental findings of Refs. 13 and 14.

When the electrons condense forming d-wave pairs, the electron scattering rate is dramatically reduced (see Fig. 1) and a V-shaped gap opens in the local one-electron density of states. The particle-hole response around (π,π) is severely reduced for frequencies below the superconducting gap. A resonance appears in the spin susceptibility coarse grained
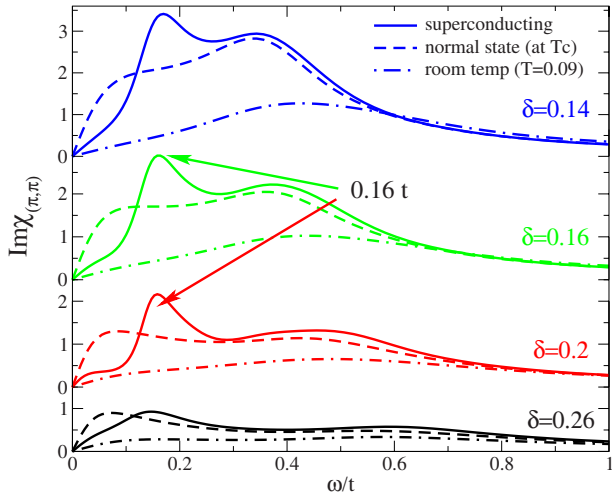
FIG. 3. (Color online) The dynamical spin susceptibility at **q** $=(\pi,\pi)$ for few different doping levels and three different temperatures: superconducting state and normal state at the transition temperature and at room temperature. The pronounced peak is formed in superconducting (SC) state at $0.16t \approx 48$ meV, and a broad peak in normal state is around $100-140$ meV. Susceptibility at normal temperature is much smaller and the peak moves to higher frequencies. The resonance is strongest at the optimally doped system. It disappears quickly in the overdoped site and somewhat more slowly in the underdoped side.

around (π,π), over $1/4$ of the Brillouin (this quantity can be compared with the **q** integrated susceptibility measured in neutron scattering of Ref. 15), at an energy scale of the order of $0.16t$, which is approximately $5T_c$ independent of temperature, as shown in Fig. 3.

In addition, the coarse grained spin response has an additional broader peak around $0.35-0.45t$, extending to very

high frequencies of order of $t \approx 300$ meV, which also gains some weight upon condensation and represents the dominant contribution to the exchange energy difference between superconducting and normal states.[6]

Pseudoparticle interpretation. We now return to a physical interpretation of the results. It turns out that out of the large number of pseudoparticles which are involved in our calculation (3^4), only four distinct pseudoparticles are very important, having the largest weight in the ground state as shown in Fig. 4. This fact suggests a convenient interpretation of our results in terms of pseudoparticles by interpreting the physical response functions in terms of convolutions of pseudoparticle Green's functions.

Underdoped regime. At small doping, the most important pseudoparticle is the singlet state with one particle per site and zero momentum (number of electrons per plaquette $N=4$, total spin of the plaquette $S=0$, and total momentum per plaquette $K=0$) (half-filled singlet). It has the largest occupancy as shown in Fig. 4(c). It describes a system locked in a short range singlet state as a consequence of the strong superexchange interaction. The electron spectral function describes the process of addition and removal of an electron from the system at frequency ω. We interpret this quantity as a convolution of two pseudoparticles with different cluster occupations N and $N+1$, or $N-1$ with integral taken between zero and ω. Note that the pseudoparticle spectral functions have thresholds, namely, a lowest energy below which their spectral weight vanishes. The necessary condition for a peak of the one-particle spectral function at the Fermi level is that at least two pseudoparticle spectral functions share common threshold and are strongly peaked at the same threshold. Since the thresholds of the other pseudoparticles are significantly shifted with reference to the half-filled singlet, a pseudogap results in the one-particle spectra in the underdoped regime. One can show that this gap in threshold ener-
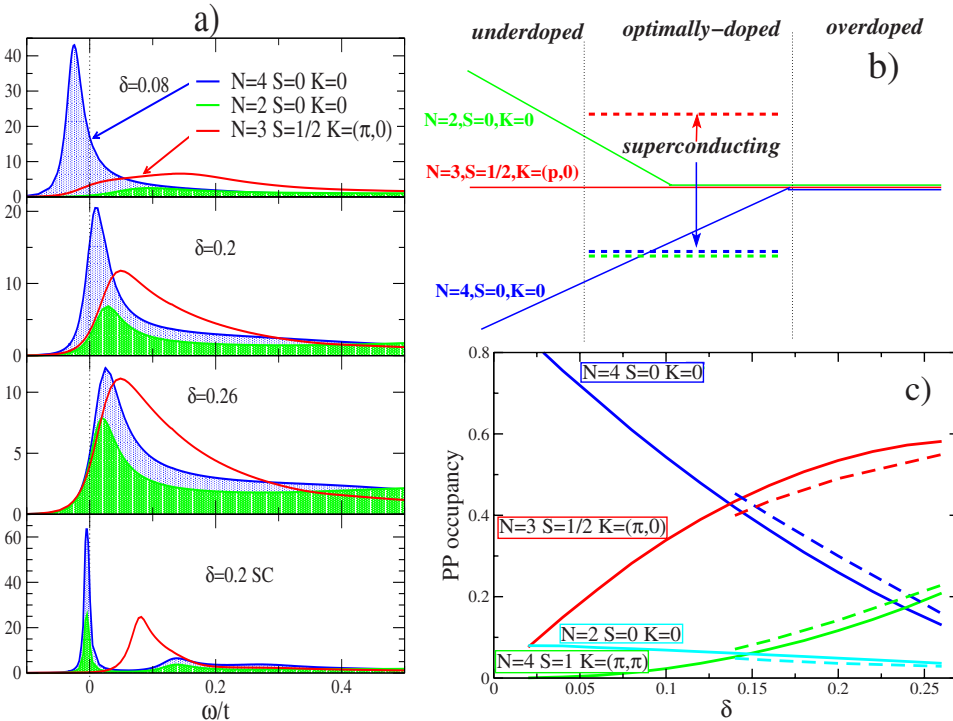

FIG. 4. (Color online) (a) Pseudoparticle spectral functions for the three most important pseudoparticles: ground states for $N=4$, $N=3$, and $N=2$ sectors. (b) Sketch of pseudoparticle threshold energies which can be interpreted as the effective many-body levels in normal and superconducting states. (c) Pseudoparticle occupancies versus doping for the most important pseudoparticles. The full lines correspond to the normal state, while the dashed lines correspond to the superconducting state.

gies severely limits the possible decay processes of the electron resulting in a low electronic scattering rate.

Overdoped regime. On the overdoped side, all three important pseudoparticles (half-filled singlet, doublet with one hole per plaquette, and singlet with two holes per plaquette) have a power law divergence at the same threshold frequency at zero temperature [Figs. 4(a) and 4(b)], which is a standard signature of the Kondo effect. Hence, the one-particle spectral function develops the Kondo-Suhl resonance peaked slightly above the Fermi level.

Transition region: Normal state. In the optimally doped region, the Kondo effect and the superexchange compete, giving rise to a regime with very large scattering rate and, consequently, a small coherence scale. In the critical region, the thresholds of the pseudoparticles (see Fig. 4) begin to merge when going from the underdoped to the overdoped regime.

The spectral function in the underdoped regime is dominated by the convolution of one $N=4$ and the doublet $N=3$ state and, hence, has more weight below the Fermi level than above it. The opposite is true in the overdoped regime. Hence, in the region around optimal doping, we have a restoration of particle-hole symmetry at low energies.

Transition into the superconducting state. The degeneracy responsible for the strongly incoherent metal with large scattering rate at the Fermi level is lifted by the superconductivity avoiding the quantum critical point. Figure 4(a) shows that both important singlet pseudoparticles (for $N=4$ and $N=2$) develop a very sharp peak at the same threshold frequency and, at the same time, their occupancy increases [see Fig. 4(c)] upon condensation, indicating that electrons are locked into singlets with zero momentum. A gap opens between the singlets and doublets, which gives the gap in the one-particle density of states. Because of this gap in the pseudoparticle thresholds, the large imaginary part of the electron self-energy does not persist in the superconducting state (see also Fig. 1). Since the density of states is composed of two almost equally important contributions, i.e., the convolution of the doublet with both singlets ($N=4$ and $N=2$),

the superconducting gap is almost particle-hole symmetric in the optimally doped regime with half-width of the order of $0.12t$. When the doping value is changed from its critical value, the asymmetry in the superconducting density of states appears. The magnitude of the asymmetry is the same as the asymmetry of the corresponding normal state spectra and comes from the fact that the occupancy and, therefore, importance of the $N=4$ half-filled singlet exceeds the importance of the $N=2$ singlet [see Fig. 4(c)]. The spin susceptibility comes almost entirely from the convolution of the half-filled singlet with the half-filled triplet [$N=4$, $S=1$, and $K=(\pi,\pi)$]. The latter develops a peak at an energy of $0.16t$ upon condensation, which causes the resonance in the spin susceptibility.

To conclude, we have identified an anomalously large scattering rate and power law correlations in the optical conductivity around the optimal doping point of the *t-J* model. These effects, which are reminiscent of the proximity to some form of criticality, are avoided or removed when electrons condense into the *d*-wave superconducting state, which restores coherence and gives rise to a resonance in the spin susceptibility.

Further explorations of these anomalies using a zero temperature method are needed to clarify further the character of the underlying criticality which separates the two distinct Fermi liquid regimes, underdoped and overdoped. This is needed to elucidate if the resulting impurity model is close to a critical point which would result in a finite temperature phase diagram similar to Fig. 1, as proposed previously by Capone *et al.* in the context of the two-band Hubbard model with inverted Hund's rule exchange.[16] There could also be a finite temperature critical end point at lower temperature, as has been found in DMFT lattice models related to the two impurity model.[17] Power laws in an intermediate asymptotic regime, without an obvious underlying quantum critical impurity model, have also been found in frustrated magnets.[18]

Another possibility is that the normal state without any unbroken symmetries cannot be continued down to zero temperature, in which case superconductivity has no normal parent state at $T=0$.

[1] A. I. Lichtenstein and M. I. Katsnelson, Phys. Rev. B **62**, R9283 (2000).

[2] M. H. Hettler, A. N. Tahvildar-Zadeh, M. Jarrell, T. Pruschke, and H. R. Krishnamurthy, Phys. Rev. B **58**, R7475 (1998).

[3] M. Civelli, M. Capone, S. S. Kancharla, O. Parcollet, and G. Kotliar, Phys. Rev. Lett. **95**, 106402 (2005).

[4] B. Kyung, S. S. Kancharla, D. Senechal, A.-M. S. Tremblay, M. Civelli, and G. Kotliar, Phys. Rev. B **73**, 165114 (2006).

[5] T. D. Stanescu and G. Kotliar, Phys. Rev. B **74**, 125110 (2006).

[6] K. Haule and G. Kotliar, Europhys. Lett. **77**, 27007 (2007).

[7] T. Maier, M. Jarrell, T. Pruschke, and M. H. Hettler, Rev. Mod. Phys. **77**, 1027 (2005).

[8] G. Kotliar, S. Y. Savrasov, K. Haule, V. S. Oudovenko, O. Parcollet, and C. A. Marianetti, Rev. Mod. Phys. **78**, 865 (2006).

[9] G. Kotliar, S. Y. Savrasov, G. Palsson, and G. Biroli, Phys. Rev. Lett. **87**, 186401 (2001).

[10] K. Haule, S. Kirchner, J. Kroha, and P. Wölfle, Phys. Rev. B **64**, 155111 (2001).

[11] P. Werner, A. Comanac, L. de Medici, M. Troyer, and A. J. Millis, Phys. Rev. Lett. **97**, 076405 (2006).

[12] K. Haule, Phys. Rev. B **75**, 155113 (2007).

[13] A. El Azrak, R. Nahoum, N. Bontemps, M. Guilloux-Viry, C. Thivet, A. Perrin, S. Labdi, Z. Z. Li, and H. Raffy, Phys. Rev. B **49**, 9846 (1994).

[14] A. El Azrak, R. Nahoum, N. Bontemps, M. Guilloux-Viry, C. Thivet, A. Perrin, S. Labdi, Z. Z. Li, and H. Raffy, Phys. Rev. B **49**, 9846 (1994); D. van der Marel, H. J. A. Molegraaf, J. Zaanen, Z. Nussinov, F. Carbone, A. Damascelli, H. Eisaki, M. Greven, P. H. Kes, and M. Li, Nature (London) **425**, 271 (2003).

[15] P. Dai, H. A. Mook, S. M. Hayden, G. Aeppli, T. G. Perring, R. D. Hunt, and F. Doan, Science **284**, 1344 (1999).

[16] M. Capone, M. Fabrizio, C. Castellani, and E. Tosatti, Phys. Rev. Lett. **93**, 047001 (2004).

[17] G. Moeller, V. Dobrosavljevic, and A. E. Ruckenstein, Phys. Rev. B **59**, 6846 (1999).

[18] A. Georges, R. Siddharthan, and S. Florens, Phys. Rev. Lett. **87**, 277203 (2001).